Proceedings of Machine Learning Research vol 242:1–10, 2024

Design of observer-based finite-time control for inductively coupled power transfer system with random gain fluctuations

T. Satheesh SATHEESHTKGM@GMAIL.COM
Department of Mathematics, Karpagam Academy of Higher Education, Coimbatore - 641021, India

R. Sakthivel KRSAKTHIVEL@BUC.EDU.IN
Department of Applied Mathematics, Bharathiar University, Coimbatore - 641046, India

Abstract

This investigation focuses on the issues of finite-time stochastic stabilisation and non fragile control design for inductively coupled power transfer systems (ICPTSs) in the presence of stochastic disturbances. Primarily, the observer system exploits the information obtained from the output of the ICPTSs to accurately reconstruct the states of the ICPTS. The observer-based non fragile control is put forward by including the estimated states of the system and gain fluctuations, which assist in achieving the desired finite-time stochastic stabilisation of the addressed system. Furthermore, via the use of Lyapunov stability theory and Ito's formula, conditions based on linear matrix inequalities are derived, which serve as adequate criteria for affirming the desired results. In conclusion, the results of the simulation that have been offered provide evidence that the proposed theoretical outcomes and control system are viable propositions.

Keywords: Inductively coupled power transfer system; Stochastic disturbance; Non-fragile control; State estimation; Finite-time stability.

1. Introduction

Wireless power transfer systems (WPTSs), covering both inductive and resonant WPTSs, have been effectively used in multiple sectors throughout the last few decades. More specifically, it's a method that facilitates two separate objects to transfer electrical energy to one another by resorting to electromagnetic induction. Academic scholars are progressively interested in it because of its reputation as a cutting-edge tool that is dependable, effective, and adaptable; it also shows potential for use in industry (Li et al. , 2019; Dai et al. , 2022). With the proliferation of user-friendly wireless technologies, inductively coupled power transfer systems (ICPTS) have recently seen a meteoric rise in popularity (Yu et al. , 2019). Specifically, this technology exhibits residue-free operation and is capable of functioning well in hazardous conditions, unaffected by external factors such as ice, water, and dirt (Dai et al. , 2016). This stands in contrast to traditional charging techniques, which lack this capability. Various causes, such as temperature fluctuations, electromagnetic interference from nearby electronic devices, load variations, and other variables, may lead to disruptions in the power system (Li et al. , 2013). Hence, it is essential to set up a robust control mechanism capable of resisting the disturbances taking place inside the system.

On a separate note, the design of a conventional controller relies essentially on the pretence that the course of action is actually exact when applied to a dynamical system. However, as the system operates throughout the industrial phase, the control parameters will experience fluctuations. These fluctuations can be triggered by untoward shifts in the operating conditions, environmental factors,

equipment malfunctions, component ageing, errors in number circulation, and actuator demise (Xu et al. , 2023). As a result, the operation's precision would be impacted. Hence, scientists endeavour to design a controller that is impervious to variations in its coefficient, leading to the emergence of a non-fragile control. Moreover, it is noteworthy that external events might potentially influence the occurrence of changes in control gain. Consequently, in this situation, fluctuations in gain can happen in a probabilistic fashion. In recent years, many remarkable research investigations have been undertaken on the occurrence of random gain variations, taking this issue into consideration (Huang et al. , 2021; Pan et al. , 2022). Taking into account these advancements, this research includes variations in the control design to enhance the ICPTSs' capacity to endure gain changes and attain the desired stabilisation.

Furthermore, the concepts of exponential and asymptotic stability elucidate the long-term dynamic behaviour of control systems. Nevertheless, in many practical situations, the spotlight is often centred on the dynamics of systems during a fixed time frame, since excessively large state values are seen as undesirable. When considering this scenario, it is of the utmost importance to investigate the transient behaviour of the system during a finite-time (FT) period (Wan et al. , 2021). As a consequence of this, the theory of FT stability is put forth, which evaluates the transient behaviour of the system and ensures that the system trajectories continue to exist within a limit that is acceptable during a brief amount of time (Zhang et al. , 2021).

Besides, from a practical standpoint, the state configuration of the system is habitually unknown or only partially known, and it is neither conveniently measurable nor easily monitorable. In such circumstances, the conventional state-feedback controller may lack the capability to provide adequate performance, resulting in system instability. To remedy this limitation, the observer approach is used, which recalibrates and estimates the system's state by means of the data from the input and output dynamics Meng et al. (20222). Following the aforementioned process, it is customary to employ state estimates of the system in a configured controller in order to effectively modulate the behaviour of the system under consideration. The concept of observer strategy has garnered significant attention within research communities due to its advantageous characteristics. Consequently, numerous noticeable findings have been documented (see Han et al. (2022) and references cited therein). In light of the notable findings derived from these groundbreaking inquiries, it is imperative to pragmatically incorporate the observer mechanism into ICPTSs, aiming to assess the dynamics of the system's state.

Building upon the aforementioned research inquiries and identified gaps, the primary objective of this study is to delve into the topic of FT stability for ICPTSs. The main contributions of this paper's research are, in brief, as follows:

- With the aid of observer-based non fragile control, the issue of FT stochastic stabilisation for ICPTSs prone to stochastic disturbances has been dealt with. Meanwhile, the observer system is structured to estimate the state of the system under scrutiny.

- Following that, an observer-based control is established by utilising the information received from the observer that is specified. On top of that, variations are included in the controller with a view to raising the controller's resilience.

- Moreover, the inquiry employs Ito's formula and the theory of Lyapunov's stability to figure out the requisite criteria in terms of linear matrix inequalities, ensuring the realisation of the primary objective.

- A numerical example is provided at the conclusion of this study, showcasing the simulation results to underline the precision and feasibility of the put-up controller.

2. Model Description and Preliminaries

This part commences by delineating an ICPTS framework. In particular, ICPTSs consist of two coupled circuits that are aided by a magnetic coupling mechanism. Through the use of space electromagnetic coupling technology, the main power source is able to transmit electricity to electrical devices without using physical contact. In addition, the circuit architecture of ICPTS has been shown in Figure 1. The LC resonant circuit on the left is referred to as the main side, while the one on the right is referred to as the secondary side. Furthermore, $\mathfrak{C}_1$ and $\mathfrak{C}_2$ stand for the capacitance of the main and secondary sides, respectively. Additionally, $\mathtt{R}_1$ and $\mathtt{R}_2$ indicate the parasitic resistance on both sides. $\mathtt{M}$ specifies the mutual inductance among the two sides, whereas $\mathtt{R}_L$ reflects the resistance of the load. $\mathtt{L}_1$ and $\mathtt{L}_2$ stand for the self-inductance. $\mathtt{u}_1(t)$, $\mathtt{i}_1(t)$, $\mathtt{u}_2(t)$, and $\mathtt{i}_2(t)$ represent the voltage and current associated with capacitance.

As stated in circuit theory, resonance in the ICPTS can only be achieved if the main and secondary sides fulfil the ensuing criteria Yu et al. (2019):

$$\mathfrak{y}_0\mathtt{L}_1 = \frac{1}{\mathfrak{y}_0\mathfrak{C}_1}, \tag{1}$$

$$\mathfrak{y}_0\mathtt{L}_2 = \frac{1}{\mathfrak{y}_0\mathfrak{C}_2}, \tag{2}$$

where $\mathfrak{y}_0$ specifies the resonant angular frequency. In addition, the analogous circuit for the ICPTSs is depicted schematically in Figure 2. The noise-perturbed framework, described in Dai et al. (2022) and Yu et al. (2019), is constructed using Kirchhoff's law. The framework is shown below:

$$\begin{cases} \mathcal{S}(t)\mathtt{E}_{\mathtt{DC}} & = \mathtt{u}_1(t) + \mathtt{i}_1(t)\mathtt{R}_1 + \mathtt{L}_1\frac{d\mathtt{i}_1}{dt} + \mathtt{M}\frac{d\mathtt{i}_2}{dt} + \mathfrak{d}_1\mathtt{i}_1(t)\mathcal{F}(t), \\ 0 & = \mathtt{L}_2\frac{d\mathtt{i}_2}{dt} + \mathtt{M}\frac{d\mathtt{i}_1}{dt} + \mathtt{i}_2(t)\mathtt{R}_2 + \mathtt{u}_2(t) + \mathtt{i}_2(t)\mathtt{R}_{\mathtt{L}} + \mathfrak{d}_2\mathtt{i}_2(t)\mathcal{F}(t), \\ \mathfrak{C}_1\frac{d\mathtt{u}_1}{dt} & = \mathtt{i}_1(t) + \mathfrak{d}_1\mathtt{i}_1(t)\mathcal{F}(t), \\ \mathfrak{C}_2\frac{d\mathtt{u}_2}{dt} & = \mathtt{i}_2(t) + \mathfrak{d}_2\mathtt{i}_2(t)\mathcal{F}(t), \end{cases} \tag{3}$$

where where $\mathcal{S}(t)$ specifies the inverter; $\mathtt{E}_{\mathtt{DC}}$ indcates input DC; $\mathfrak{d}_1$ and $\mathfrak{d}_2$ stand for the noise intensity; $\mathcal{F}(t)$ symbolizes the Gauss process.

2.1. State Space Modeling of ICPT System

By using the prior differential equations, the ensuing state space representation of the ICPTSs is provided, taking into account stochastic disturbances:

$$\begin{aligned} d\rho(t) =& \mathcal{C}\rho(t)dt + \mathcal{D}c(t)dt + \mathcal{E}\rho(t)d\delta(t), \\ \alpha(t) =& \mathcal{G}\rho(t), \end{aligned} \tag{4}$$

where $\rho(t)$ is the state vector and $\rho(t) = [\mathtt{i}_1(t)\ \mathtt{u}_1(t)\ \mathtt{i}_2(t)\ \mathtt{u}_2(t)]$; $c(t)$ stands for the control input; $\delta(t)$ indicates n-dimensional Wiener process; $\mathcal{C}$, $\mathcal{D}$ and $\mathcal{E}$ symbilize the real matrices and their form

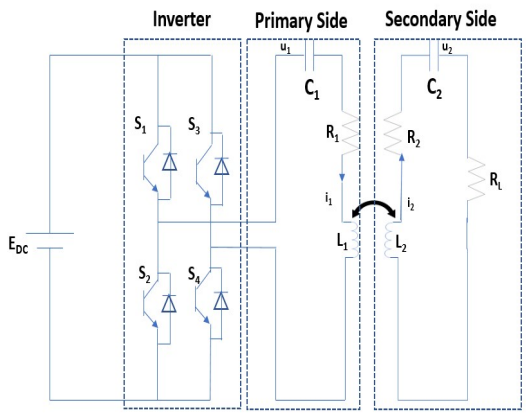

Figure 1: Circuit topology Dai et al. (2022) and Yu et al. (2019)

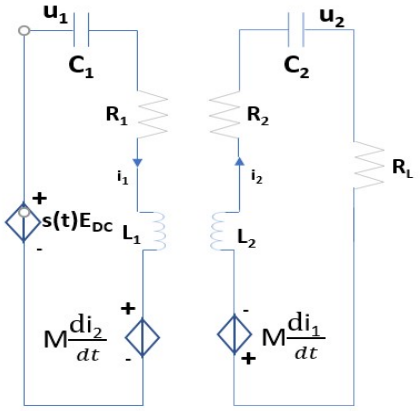

Figure 2: Equivalent circuit Dai et al. (2022) and Yu et al. (2019)

is presented hereunder:

$$\mathcal{C} = \begin{bmatrix} \frac{R_1L_2}{M^2-L_1L_2} & \frac{L_2}{M^2-L_1L_2} & \frac{(R_2+R_L)M}{L_1L_2-M^2} & \frac{M}{L_1L_2-M^2} \\ \frac{1}{\mathfrak{C}_1} & 0 & 0 & 0 \\ \frac{R_1M}{L_1L_2-M^2} & \frac{M}{L_1L_2-M^2} & \frac{(R_2+R_L)L_1}{M^2-L_1L_2} & \frac{L_1}{M^2-L_1L_2} \\ 0 & 0 & \frac{1}{\mathfrak{C}_2} & 0 \end{bmatrix}, \mathcal{D} = \begin{bmatrix} \frac{L_2}{L_1L_2-M^2} & 0 & \frac{M}{M^2-L_1L_2} & 0 \end{bmatrix}^T \text{ and}$$

$$\mathcal{E} = \begin{bmatrix} -\mathfrak{d}_1 & 0 & \frac{M}{L_2} & 0 \\ \frac{\mathfrak{d}_1}{\mathfrak{C}_1} & 0 & 0 & 0 \\ \frac{M}{L_1L_2-M^2} & 0 & \frac{L_1\mathfrak{d}_2}{M^2-L_1L_2} & 0 \\ 0 & 0 & \frac{\mathfrak{d}_2}{\mathfrak{C}_2} & 0 \end{bmatrix}.$$

2.2. Configuration of observer System

It is crucial to note that in the context of studying dynamical systems, there are instances when it is impossible to possess comprehensive insight into the system states. And, with the intent to measure the system state, the observer system is framed, and its state space representation is offered below:

$$d\hat{\rho}(t) = \big[\mathcal{C}\hat{\rho}(t) + \mathcal{D}c(t) + \mathcal{H}(\alpha(t) - \hat{\alpha}(t))\big]dt, \tag{5}$$

$$\hat{\alpha}(t) = \mathcal{G}\hat{\rho}(t), \tag{6}$$

where $\hat{\rho}(t)$ and $\hat{\alpha}(t)$ symbolize the estimation of $\rho(t)$ and $\alpha(t)$, respectively; $\mathcal{H}$ indicate the gain matrices of observer model.

2.3. Control Configuration

Moreover, while setting up robust controllers for real-time systems, it is crucial to keep in mind that the gain parameters of the controller can vary due to many factors. Hence, it is essential to develop a controller that can withstand a certain degree of fluctuation linked to its gain value. Taking this into

consideration, an observer-based non fragile control that has the following structure has sprouted up:

$$c(t) = (\mathcal{P} + \mathfrak{g}(t)\Delta\mathcal{P}(t))\hat{\rho}(t), \tag{7}$$

where $\mathcal{P}$ indicates the gain matrix of the controller which will be reckoned thereafter. $\Delta\mathcal{P}(t)$ is the fluctuations in the control segment and it has the frame $\Delta\mathcal{P}(t) = \mathcal{A}\varkappa(t)\mathcal{B}$ in which $\mathcal{A}$ and $\mathcal{B}$ are known real matrices and $\varkappa(t)$ satisfies the frame $\varkappa^T(t)\varkappa(t) < I$. $\mathfrak{g}(t)$ signifies the stochastic variables satisfy the relations $Prob\{\mathfrak{g}(t) = 1\} = \mathbb{E}\{\mathfrak{g}(t)\} = \bar{\mathfrak{g}}$, $Prob\{\mathfrak{g}(t) = 0\} = 1 - \mathbb{E}\{\mathfrak{g}(t)\} = 1 - \bar{\mathfrak{g}}$, for given scalar $\bar{\mathfrak{g}} \in [0, 1]$.

Subsequently, by setting up the error system $\kappa(t) = \rho(t) - \hat{\rho}(t)$ and altering the control (7), we can promptly gain the subsequent set of equations:

$$\begin{aligned} d\rho(t) =& [\mathcal{C}\rho(t) + \mathcal{D}[\mathcal{P} + \mathfrak{g}(t)\Delta\mathcal{P}(t)]\hat{\rho}(t)]dt + \mathcal{E}\rho(t)d\delta(t), \\ d\kappa(t) =& \big[[\mathcal{C} - \mathcal{H}\mathcal{G}]\kappa(t) - \mathcal{H}\digamma\mathcal{G}\rho(t)\big]dt + \mathcal{E}\rho(t)d\delta(t). \end{aligned} \tag{8}$$

To streamline the scrutiny, the equation (8) can be modified in an appropriate way, as shown below:

$$\begin{cases} d\rho(t) = & \tau_1(t)dt + \theta_1(t)d\delta(t), \\ d\kappa(t) = & \tau_2(t)dt + \theta_1(t)d\delta(t), \end{cases} \tag{9}$$

where $\theta_1(t) = \mathcal{E}\rho(t)$; $\tau_1(t)$, $\tau_2(t)$ is the terms before dt in relation (8).

3. Main Results

This section will emphasise showcasing the FT stochastic stabilisation of ICPTSs via the implementation of the observer-based non-fragile control specified in the former section.

Theorem 1 *For given scalars $\mathfrak{p} > 0$, $\bar{\mathfrak{g}} \in [0, 1]$ and matrix $\mathcal{K} > 0$, the ICPTS (4) is FT stochastically stabilized via the observer-based non fragile control (7), if the scalars $\mathfrak{q} > 0$, $\mathfrak{s}_1 > 0$, $\mathfrak{s}_2 > 0$ and matrices $\mathcal{J} > 0$, $\mathcal{M}$, $\mathcal{N}$, $\breve{\mathcal{J}}$ exist, such that the ensuing conditions are met:*

$$[\beth] < 0, \tag{10}$$

$$\begin{bmatrix} -\mathfrak{q} & (\mathcal{J}\mathcal{D} - \mathcal{D}\bar{\mathcal{J}})^T \\ * & -\mathcal{I} \end{bmatrix} < 0 \tag{11}$$

$$e^{\mathfrak{p}\mathfrak{T}_u} 2\mathfrak{v}_1\mathfrak{m}_1 < \mathfrak{z}_1\mathfrak{m}_1, \tag{12}$$

$\beth^a_{1,1} = sym\{\mathcal{J}\mathcal{C} + \mathcal{D}\mathcal{M}\} + \mathcal{E}^T\mathcal{J}\mathcal{E} + \mathcal{E}^T\mathcal{J}\mathcal{E} - \mathfrak{p}\mathcal{J}$, $\beth^a_{1,2} = -\mathcal{D}\mathcal{M}$, $\beth^a_{1,3} = \bar{\mathfrak{g}}\mathcal{D}\breve{\mathcal{J}}\mathcal{A}$, $\beth^a_{1,4} = \mathfrak{s}_1\mathcal{B}^T$, $\beth^a_{1,5} = \bar{\mathfrak{g}}\mathcal{D}\breve{\mathcal{J}}\mathcal{A}$, $\beth^a_{2,2} = sym\{\mathcal{J}\mathcal{C} - \mathcal{N}\mathcal{G}\} - \mathfrak{p}\mathcal{J}$, $\beth^a_{2,6} = \mathfrak{s}_2\mathcal{B}^T$, $\beth^a_{3,3} = -\mathfrak{s}_1\mathcal{I}$, $\beth^a_{4,4} = -\mathfrak{s}_1\mathcal{I}$, $\beth^a_{5,5} = -\mathfrak{s}_2\mathcal{I}$ and $\beth^a_{6,6} = -\mathfrak{s}_2\mathcal{I}$. Moreover, the gain matrices can be reckoned utilizing the relation $\mathcal{P} = \bar{\mathcal{J}}^{-1}\mathcal{M}$ and $\mathcal{H} = \mathcal{J}^{-1}\mathcal{N}$.*

Proof *We have used Lyapunov stability theory as a means to prove this thesis. Further, pursuant to equation (9), the Lyapunov function is stated as follows:*

$$\mathfrak{V}(t) = \rho^T(t)\mathcal{J}\rho(t) + \kappa^T(t)\mathcal{J}\kappa(t). \tag{13}$$

In the meantime, complying with Ito's formula, we acquire the following relation:

$$d\mathfrak{V}(t) = \mathcal{L}\mathfrak{V}(t)dt + \rho^T(t)\mathcal{J}\theta_1(t)d\delta(t) + \rho^T(t)\mathcal{J}\theta_1(t)d\delta(t), \tag{14}$$

Subsequently, in line with (9), the infinitesimal operator $\mathcal{L}$ can be reckoned as

$$\begin{aligned}
\mathbb{E}\{\mathcal{L}\mathfrak{V}(t)\} =& \mathbb{E}\Bigg\{\frac{\partial\mathfrak{V}(t)}{\partial t} + \frac{\partial\mathfrak{V}(t)}{\partial\rho(t)}\tau_1(t) + \frac{\partial\mathfrak{V}(t)}{\partial\kappa(t)}\tau_2(t) + \frac{1}{2}\left(\theta_1^T(t)\frac{\partial^2\mathfrak{V}(t)}{\partial^2\rho(t)}\theta_1(t)\right) \\
&+ \frac{1}{2}\left(\theta_1^T(t)\frac{\partial^2\mathfrak{V}(t)}{\partial^2\rho(t)}\theta_1(t)\right)\Bigg\} \\
=& \mathbb{E}\Bigg\{sym(\rho^T(t)\mathcal{J}\tau_1(t)) + sym(\kappa^T(t)\mathcal{J}\tau_2(t)) + \theta_1^T(t)\mathcal{J}\theta_1(t) \\
&+ \theta_1^T(t)\mathcal{J}\theta_1(t)\Bigg\} \\
=& \mathbb{E}\Bigg\{\big[\mathcal{C}\rho(t) + \mathcal{D}(\mathcal{P} + \mathfrak{g}(t)\Delta\mathcal{P}(t))\hat{\rho}(t)\big]^T\mathcal{J}\big[\mathcal{C}\rho(t) + \mathcal{D}(\mathcal{P} + \mathfrak{g}(t)\Delta\mathcal{P}(t))\hat{\rho}(t)\big] \\
&+ \big[(\mathcal{C} - \mathcal{H}\mathcal{G})\kappa(t) - \mathcal{D}\rho_P(t)\big]^T\mathcal{J}\big[(\mathcal{C} - \mathcal{H}\mathcal{G})\kappa(t) - \mathcal{D}\rho_P(t)\big] \\
&+ \rho^T(t)\mathcal{E}^T\mathcal{J}\mathcal{E}\rho(t) + \rho^T(t)\mathcal{E}^T\mathcal{J}\mathcal{E}\rho(t)\Bigg\}.
\end{aligned} \tag{15}$$

In the subsequent phase, the aforesaid equation can be organised and put forward in the following way:

$$\mathbb{E}\{\mathcal{L}\mathfrak{V}(t) + \mathfrak{p}\mathfrak{V}(t)\} = \mathfrak{x}^T(t)[\breve{\aleph}]\mathfrak{x}(t), \tag{16}$$

where $\mathfrak{x}^T(t) = \begin{bmatrix}\rho^T(t) & \kappa^T(t)\end{bmatrix}$, $\breve{\aleph}_{1,1} = sym\{\mathcal{J}\mathcal{C} + \mathcal{J}\mathcal{D}(\mathcal{P} + \bar{\mathfrak{g}}\Delta\mathcal{P}(t))\} + \mathcal{E}^T\mathcal{J}\mathcal{E} + \mathcal{E}^T\mathcal{J}\mathcal{E} - \mathfrak{p}\mathcal{J}$, $\breve{\aleph}_{1,2} = -\mathcal{J}\mathcal{D}(\mathcal{P} + \bar{\mathfrak{g}}\Delta\mathcal{P}(t))$, $\breve{\aleph}_{2,2} = sym\{\mathcal{J}\mathcal{C} - \mathcal{J}\mathcal{H}\mathcal{G}\} - \mathfrak{p}\mathcal{J}$,

Furthermore, conditions $\mathcal{J}\mathcal{D} = \mathcal{D}\bar{\mathcal{J}}$, $\bar{\mathcal{J}}\mathcal{P} = \mathcal{M}$, $\mathcal{J}\mathcal{H} = \mathcal{N}$ are applied to the matrix $[\breve{\aleph}]$ to circumvent the nonlinearities that emerge as a result of the premise of unknown gain matrices. Subsequent to this, by applying the Schur complement lemma to the resultant matrix, we grab the matrix $\beth$ states in the relation (10). Moreover, if the requisite laid out in inequality (10) is satisfied, then we have the criterion $\mathbb{E}\{\mathcal{L}\mathfrak{V}(t) + \mathfrak{p}\mathfrak{V}(t)\} < 0$. Therefore, on the basis of the Lyapunov stability theory, we can deduce that the system (9) being investigated is stochastically stable. Therein, it is important to note that the condition $\mathcal{J}\mathcal{D} = \mathcal{D}\bar{\mathcal{J}}$ can be equitably written as (11) since it is not a strict linear matrix inequality.

The subsequent phase involves the demonstration of FT stability. To address this objective, we integrate the inequality $\mathbb{E}\{\mathcal{L}\mathfrak{V}(t) + \mathfrak{p}\mathfrak{V}(t)\} < 0$ across the interval from 0 to $\mathfrak{T}_u$. Consequently, we obtain

$$e^{-\mathfrak{p}\mathfrak{T}_u}\mathbb{E}\{\mathfrak{V}(t)\} - \mathbb{E}\{\mathfrak{V}(0)\} < 0 \implies \mathbb{E}\{\mathfrak{V}(t)\} < e^{\mathfrak{p}\mathfrak{T}_u}\mathbb{E}\{\mathfrak{V}(0)\}. \tag{17}$$

Apart from that, using a presumption $\breve{\mathcal{J}} = \mathcal{K}_1^{-\frac{1}{2}}\mathcal{J}\mathcal{K}_1^{-\frac{1}{2}}$, we can readily derive the ensuing set of relations for real matrices $\mathcal{K}_1 > 0$ and $\mathcal{K}_2 > 0$:

$$\begin{aligned}
\mathbb{E}\{\mathfrak{V}(t)\} \geq \mathbb{E}\{\rho^T(t)\mathcal{J}\rho(t)\} =& \rho^T(t)\mathcal{K}^{\frac{1}{2}}\breve{\mathcal{J}}\mathcal{K}^{\frac{1}{2}}\rho(t) \\
\geq& \mathfrak{z}_{min}(\breve{\mathcal{J}})\rho^T(t)\mathcal{K}\rho(t) \\
=& \mathfrak{z}_1\rho^T(t)\mathcal{K}\rho(t).
\end{aligned} \tag{18}$$

$\mathtt{R}_1$	$\mathtt{R}_2$	$\mathtt{L}_1$	$\mathtt{L}_2$	$\mathfrak{C}_1$	$\mathfrak{C}_2$	$\mathtt{R}_L$	$\mathtt{M}$	$\mathfrak{d}_1$	$\mathfrak{d}_2$
0.2Ω	0.2Ω	$127\mu H$	$127\mu H$	$2\mu F$	$2\mu F$	100	40	0.1	0.1

Table 1: Parameters

At the same time, it can be deduced from the onset of the Lyapunov function (13) that

$$\begin{aligned}\mathbb{E}\{\mathfrak{V}(0)\} =& \rho^T(0)\mathcal{J}\rho(0) + \kappa^T(0)\mathcal{J}\kappa(0)\\ \leq& \mathfrak{z}_{max}(\breve{\mathcal{J}})\rho^T(0)\mathcal{K}\rho(0) + \mathfrak{z}_{max}(\breve{\mathcal{J}})\kappa^T(0)\mathcal{K}\kappa(0)\\ \leq& (\mathfrak{z}_1\rho^T(0)\mathcal{K}\rho(0) + \mathfrak{z}_1\kappa^T(0)\mathcal{K}\kappa(0))\\ \leq& 2\mathfrak{z}_1\dagger_1\\ =& \varrho\dagger_1. \end{aligned} \tag{19}$$

Further, the subsequent inequality can be readily depicted by means of the constraints (17)-(19):

$$\mathbb{E}\{\rho^T(t)\mathcal{K}\rho(t)\} \leq \frac{\mathbb{E}\{\mathfrak{V}(t)\}}{\mathfrak{z}_1} = \frac{e^{\mathfrak{p}\mathfrak{T}_{\mathfrak{u}}}\varrho\dagger_1}{\mathfrak{z}_1}. \tag{20}$$

If the specifications set out in equation (12) are met, we could speculate from previous equation (20) that $\mathbb{E}\{\rho^T(t)\mathcal{K}\rho(t)\} < \dagger_2$. Hence, by taking into account Definition 2 in Xiang et al. (2012), we have determined that the ICPTS (9) is stochastically stable in the sense of FT. And with that, the demonstration of the theorem has ended. ■

Remark 2 *The observer-based finite-time control technique that has been developed has significant prospects for being utilized in higher-dimensional inductively coupled power transfer systems. The control technique exhibits efficacy in preserving stability and attaining intended performance, even in systems with elevated complexity. Nevertheless, it is crucial to recognize that as the complexity and dimension of the system increases, the computing requirements for applying the control strategy also increase. Therefore, while the methods hold relevance for higher dimensional systems, careful consideration of computational resources and efficiency becomes imperative for practical implementation.*

4. Simulation Verification

This section employs simulation results in a bid to corroborate the theoretical insights laid out in the sections preceding it. Furthermore, the system parameters have been gathered from the work Yu et al. (2019) and are depicted in Table 1. In addition, the relevant parameters for the FT theory have been set as $\dagger_1 = 2.5$, $\dagger_2 = 8$, $\mathfrak{p} = 1$, $\mathcal{K} = \mathtt{I}$ and $\mathfrak{T}_{\mathfrak{u}} = 10$. The matrices associated with the gain variations are handpicked as $\mathcal{A} = 0.01$ and $\mathcal{B} = \begin{bmatrix}0.1 & 0.2 & 0.1 & 0.2\end{bmatrix}$. Subsequently, we used the MATLAB programme to resolve the constraints produced in Theorem 1 using the prior supplied inputs, resulting in the acquisition of viable solutions. Following that, Table 2 displays the gain matrices, which are calculated using the viable solutions as input.

In order to progress, the initial conditions are picked as

$$\rho(0) = \begin{bmatrix}0.002 & -0.0011 & 0.0011 & -0.0011\end{bmatrix}^T \text{ and } \hat{\rho}(0) = \begin{bmatrix}0.002 & -0.0011 & 0.0011 & -0.0011\end{bmatrix}^T.$$

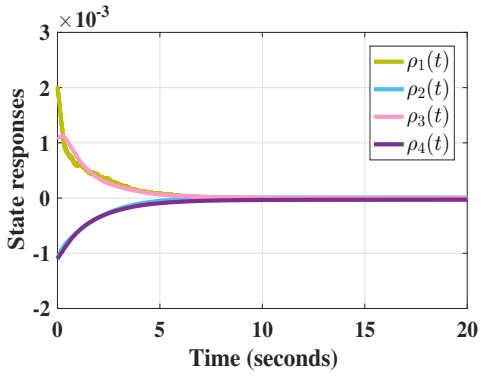

Figure 3: System response under developed controller

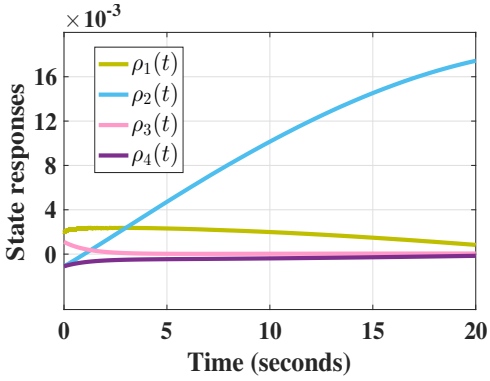

Figure 4: System response in the absence of controller

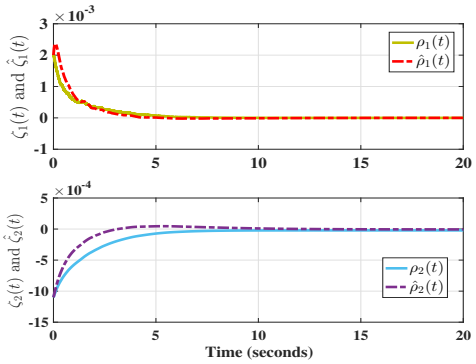

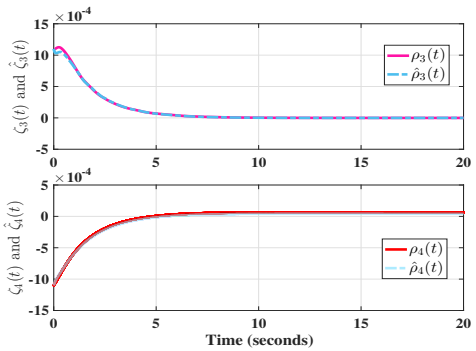

Figure 5: State and its estimation

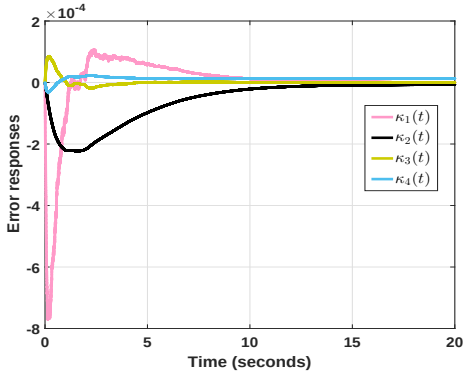

Figure 6: Evolution of estimation error

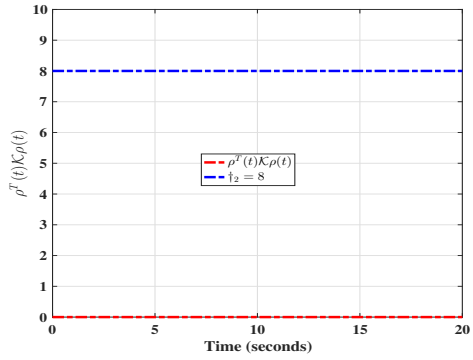

Figure 7: Time profile of $\rho^T(t)\mathcal{K}\rho(t)$

After considering the stated parameters, the simulations were carried out, and the resulting outputs are shown in Figures 3-8. To be more specific, Figures 3 and 4 show the outcome of state trajectories with and without a controller. Within, it is obvious that the system's performance

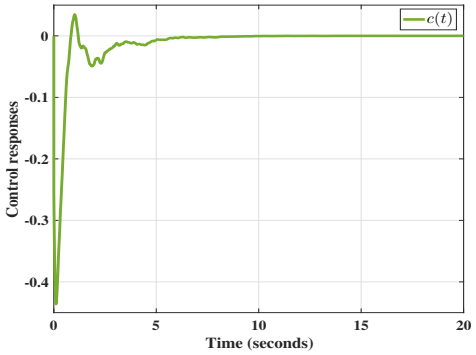

Figure 8: Control trajectories

$\mathcal{P}$	$\mathcal{H}$
$\begin{bmatrix} 300.3177 \\ -247.3975 \\ 47.9729 \\ -45.0561 \end{bmatrix}^T$	$\begin{bmatrix} 2.2467 \\ 0.0849 \\ -0.2254 \\ 0.1095 \end{bmatrix}$

Table 2: Gain matrices

improves with the built controller compared to the absence of the controller. Even more so, Figure 5 displays the outcomes of the state estimate. In this case, it is trivial to witness and prove that the observer states exactly mirror the ICPTS states in a short amount of time. Furthermore, the results of the state estimation error are shown in Figure 6, where it is clear that the estimate error decreases and eventually reaches zero as time goes on. Despite this, Figure 7 displays the trajectory of $\rho^T(t)\mathcal{K}\rho(t)$ when the controller is applied, serving as evidence of the FT stochastic stability of the ICPTSs. More precisely, it can be seen that the value of $\rho^T(t)\mathcal{K}\rho(t)$ stays below the specified threshold of $\dagger_2$. At the end, a pictorial illustration of control trajectories is provided in Figure 8.

Overall, the simulations reveal that the set up observer-based non fragile control effectively ensures the desired FT stochastic stability and accurate state estimation performance in the presence of stochastic disturbances and variations in gain matrices.

5. Conclusion

During this phase of this inquiry, an observer-based non fragile control scheme has been built for ICPTSs operating in environments with stochastic disturbances and gain fluctuations. Specifically, an observer system has been set up to quantify the state dynamics of the ICPTSs in light of the output of the system. Moreover, incorporating an uncertainty part into the controller's gain matrix also raises its resilience, which in turn delivers better performance. Subsequently, by melding Lyapunov stability theory with convex optimisation techniques, we have gleaned sufficient conditions in the form of linear matrix inequalities that ensures the desired FT stochastic stability of the examined ICPTSs, and centred on these ailments, the gain matrices can be computed. Ultimately, we verify the reliance and viable perks of the configured observer-based non fragile control through the analysis of simulation results.

References

X. Li, F. Zheng, H. Wang, X. Dai, Y. Sun and J. Hu, Analysis and design of a cost-effective single-input and regulatable multioutput WPT system, IEEE Transactions on Power Electronics, 38 (2023) 6939-6944.

X. Dai, X. Hua, S. Sun and Y. Sun, Dynamic output feedback control for wireless power transfer systems, Asian Journal of Control, DOI:https://doi.org/10.1002/asjc.3061

Z. Yu, Y. Sun, X. Dai and Z. Ye, Stability and control of uncertain ICPT system considering time-varying delay and stochastic disturbance, International Journal of Robust and Nonlinear Control, 29 (2019) 6582-6604.

X. Dai, L. Li, X. Yu, Y. Li and Y. Sun, A novel multi-degree freedom power pickup mechanism for inductively coupled power transfer system, IEEE Transactions on Magnetics, 53 (2016) 1-7.

Y.L. Li, Y. Sun and X. Dai, Robust control for an uncertain LCL resonant ICPT system using LMI method, Control Engineering Practice, 21 (2013) 31-41.

Y. Xu, S. Chai, P. Shi, B. Zhang and Y. Wang, Resilient and event-triggered control of stochastic jump systems under deception and denial of service attacks, International Journal of Robust and Nonlinear Control, 33 (2023) 1821-1837.

C. Huang and H.R. Karimi, Non-fragile $\mathtt{H}_\infty$ control for LPV-based CACC systems subject to denial-of-service attacks, IET Control Theory & Applications, 15 (2021) 1246-1256.

Y. Pan, Y. Wu and H.K. Lam, Security-based fuzzy control for nonlinear networked control systems with DoS attacks via a resilient event-triggered scheme, IEEE Transactions on Fuzzy Systems, 30 (2022) 4359-4368.

H. Wan, H.R. Karimi, X. Luan and F. Liu, Self-triggered finite-time $\mathtt{H}_\infty$ control for Markov jump systems with multiple frequency ranges performance, Information Sciences, 581 (2021) 694-710.

L. Zhang, Y. Sun, H.K. Lam, H. Li, J. Wang and D. Hou, Guaranteed cost control for interval type-2 fuzzy semi-Markov switching systems within a finite-time interval, IEEE Transactions on Fuzzy Systems, 30 (2021) 2583-2594.

X. Meng, C. Gao, B. Jiang and H.R. Karimi, Observer-based SMC for stochastic systems with disturbance driven by fractional Brownian motion, Discrete and Continuous Dynamical Systems-S, 15 (2022) 3261-3274.

J. Han, X. Liu, X. Wei and S. Sun, A dynamic proportional-integral observer-based nonlinear fault-tolerant controller design for nonlinear system with partially unknown dynamic, IEEE Transactions on Systems, Man, and Cybernetics: Systems, 52 (2022) 5092-5104.

M. Wu, F. Gao, P. Yu, J. She and W. Cao, Improve disturbance-rejection performance for an equivalent-input-disturbance-based control system by incorporating a proportional-integral observer, IEEE Transactions on Industrial Electronics, 67 (2020) 1254-1260.

Z. Xiang, C. Qiao and M.S. Mahmoud, Finite-time analysis and $\mathtt{H}_\infty$ control for switched stochastic systems, Journal of the Franklin Institute, 349 (2012) 915-927.